

Interaction of Asn105 with the Retinal Chromophore during Photoisomerization of *pharaonis* Phoborhodopsin[†]

Hideki Kandori,^{*,‡,§} Kazumi Shimono,^{||} Yoshinori Shichida,[§] and Naoki Kamo^{||}

Department of Applied Chemistry, Nagoya Institute of Technology, Showa-ku, Nagoya 466-8555, Japan,
Department of Biophysics, Graduate School of Science, Kyoto University, Sakyo-ku, Kyoto 606-8502, Japan, and
Laboratory of Biophysical Chemistry, Graduate School of Pharmaceutical Sciences, Hokkaido University,
Sapporo 060-0812, Japan

Received November 20, 2001; Revised Manuscript Received February 5, 2002

ABSTRACT: *pharaonis* phoborhodopsin (ppR; also called *pharaonis* sensory rhodopsin II, psR-II) is a photoreceptor for negative phototaxis in *Natronobacterium pharaonis*. ppR has a blue-shifted absorption spectrum with a spectral shoulder, which is highly unique for the archaeal rhodopsin family. The primary reaction of ppR is a cis–trans photoisomerization of the retinal chromophore to form the K intermediate, like the well-studied proton pump bacteriorhodopsin (BR). Recent comparative FTIR spectroscopy of the K states in ppR and BR revealed that more extended structural changes take place in ppR than in BR with respect to chromophore distortion and protein structural changes [Kandori, H., Shimono, K., Sudo, Y., Iwamoto, M., Shichida, Y., and Kamo, N. (2001) *Biochemistry* 40, 9238–9246]. FTIR spectroscopy of the N105D mutant protein reported here assigns the vibrational bands at 1704 and 1700 cm^{−1} as C=O stretches of Asn105 in ppR and ppR_K, respectively. A comparative investigation between ppR and BR further reveals that the structure at position 105 in ppR is similar to that of the corresponding position (Asp115) in BR; this observation is supported by the recent X-ray crystallographic structures of ppR [Luecke, H., Schobert, B., Lanyi, J. K., Spudich, E. N., and Spudich, J. L. (2001) *Science* 293, 1499–1503; Royant, A., Nollert, P., Edman, K., Neutze, R., Landau, E. M., Pebay-Peyroulla, E., and Navarro, J. (2001) *Proc. Natl. Acad. Sci. U.S.A.* 98, 10131–10136]. Nevertheless, structural changes upon photoisomerization at position 105 in ppR are greater than those at position 115 in BR. As a consequence of a unique chromophore–protein interaction in ppR, extended protein structural changes accompanying retinal photoisomerization occur, and these include Asn105 which is ~7 Å from the retinal chromophore.

Phoborhodopsin (pR)¹ from *Halobacterium salinarum* and *pharaonis* phoborhodopsin (ppR) from *Natronobacterium pharaonis* are members of the archaeal rhodopsins (1, 2).² pR and ppR activate cognate transducer proteins upon light absorption, leading to negative phototaxis. They possess a retinal chromophore that is embedded in one of seven transmembrane helices, like the well-studied proton pump protein bacteriorhodopsin (BR) (1–3). In the case of ppR or BR, the retinal forms a Schiff base linkage with Lys205 or Lys216, respectively, and the protonated Schiff base is

stabilized by a negatively charged counterion, Asp75 or Asp85, respectively. Light absorption triggers cis–trans photoisomerization of the retinal chromophore on formation of the K intermediate, which eventually leads to functional processes during their photocycles. A proton-transfer reaction also takes place from the Schiff base to the counterion on formation of the M intermediate.

Despite this similarity, ppR has characteristics different from those of BR. The static characteristics involve considering the spectral blue shift, the vibrational fine structure, and the isomer selectivity. The absorption maximum of ppR (500 nm) is considerably blue-shifted from that of BR (570 nm), and the absorption spectrum has a characteristic vibrational feature (1, 2). The chromophore configuration in the dark state is completely all-trans in ppR (4) as well as pR (5), whereas BR has both all-trans and 13-cis forms. In addition, differences between ppR and BR are seen in the dynamical aspects: (i) photocycling rate, (ii) stability of the K intermediate, and (iii) proton pump. The photocycle time of ppR is also ~2 orders of magnitude longer than that of BR (6, 7). It is known that ppR_K is highly stable and that ppR_L is not trapped at low temperatures (8, 9). In the absence of a transducer, ppR can pump a proton like BR (10, 11), whereas the pump efficiency is much lower than that of BR (11, 12).

[†] This work was supported in part by grants from the Japanese Ministry of Education, Culture, Sports, Science and Technology and by the Human Frontier Science Program.

* To whom correspondence should be addressed. Phone and fax: 81-52-735-5207. E-mail: kandori@ach.nitech.ac.jp.

[‡] Nagoya Institute of Technology.

[§] Kyoto University.

^{||} Hokkaido University.

¹ Abbreviations: pR, phoborhodopsin; ppR, *pharaonis* phoborhodopsin; BR, bacteriorhodopsin; BR_K, K intermediate of BR; BR_L, L intermediate of BR; BR_M, M intermediate of BR; ppR_K, K intermediate of *pharaonis* phoborhodopsin; ppR_L, L intermediate of *pharaonis* phoborhodopsin; ppR_M, M intermediate of *pharaonis* phoborhodopsin; ppR_O, O intermediate of *pharaonis* phoborhodopsin; FTIR, Fourier transform infrared; DM, *n*-dodecyl β-D-maltoside; PC, L-α-phosphatidylcholine; HOOP, hydrogen out-of-plane.

² pR and ppR are also called sensory rhodopsin-II (sR-II) and *pharaonis* sensory rhodopsin-II (psR-II), respectively.

These differences are presumably facilitated by the surrounding protein environment. Recent electron microscopy at a 6.9 Å resolution revealed that the arrangement of helices in *ppR* is very similar to that of BR (13). Therefore, their functional differences must originate from each fine structure. We recently started an investigation to compare structure and structural changes between *ppR* and BR by means of low-temperature FTIR spectroscopy. Vibrational analysis is highly sensitive to changes in molecular structure accompanying the functional processes of *ppR* and BR. Our first report on the structural changes upon photoisomerization provided common and different infrared spectral features between *ppR* and BR (14). The spectral comparison suggested that the chromophore structure is similar at the center (polyene chain), but different at both ends (β -ionone ring and the Schiff base regions). Photoisomerization in *ppR* appears to drive the motion of the Schiff base like BR. Nevertheless, the structure of the K state after photoisomerization is very different for *ppR* and BR. In BR, the chromophore distortion is localized in the Schiff base region, as shown in its hydrogen out-of-plane vibrations. In contrast, more extended structural changes take place in *ppR* in view of chromophore distortion and protein structural changes. Such a structure of the K intermediate of *ppR* is probably correlated with its high thermal stability, where almost identical infrared spectra are obtained between 77 and 170 K in *ppR* (14).

In this report, we assign one of the characteristic vibrational bands in the *ppR*_K minus *ppR* spectra. By using mutant proteins, vibrational bands at 1704 and 1700 cm^{-1} were assigned as the C=O stretches of Asn105 in *ppR* and *ppR*_K, respectively. Comparative investigation between *ppR* and BR further revealed that the structure at position 105 in *ppR* is similar to that of the corresponding position (Asp115) in BR. In contrast, structural changes upon photoisomerization at position 105 in *ppR* are greater than those at position 115 in BR. A unique chromophore–protein interaction in *ppR* presumably yields extended protein structural changes accompanying retinal photoisomerization, which includes Asn105 even at a distance of ~ 7 Å from the retinal chromophore.

MATERIALS AND METHODS

The wild-type and N105D mutant proteins of *ppR* were prepared as described previously (14–16). Briefly, the *ppR* proteins possessing a histidine tag at the C-terminus were expressed in *Escherichia coli*, solubilized with 1.5% *n*-dodecyl β -D-maltoside (DM), and purified with a Ni column. The purified *ppR* sample was then reconstituted into L- α -phosphatidylcholine (PC) liposomes by dialysis, where the molar ratio of the added PC was 50 times that of *ppR*. The mutated gene for D115N of BR was constructed and introduced into *H. salinarum* as described previously (17). The purple membranes of the wild-type and D115N mutant proteins were isolated by the method of Oesterhelt and Stoekenius (18).

FTIR spectroscopy was carried out as described previously (19). The *ppR* sample (80 μL) in 2 mM phosphate buffer (pH 7.0) was dried on a BaF₂ window with a diameter of 18 mm. After hydration by H₂O, or D₂O, the sample was mounted in an Oxford DN-1704 cryostat, and cooled to 77

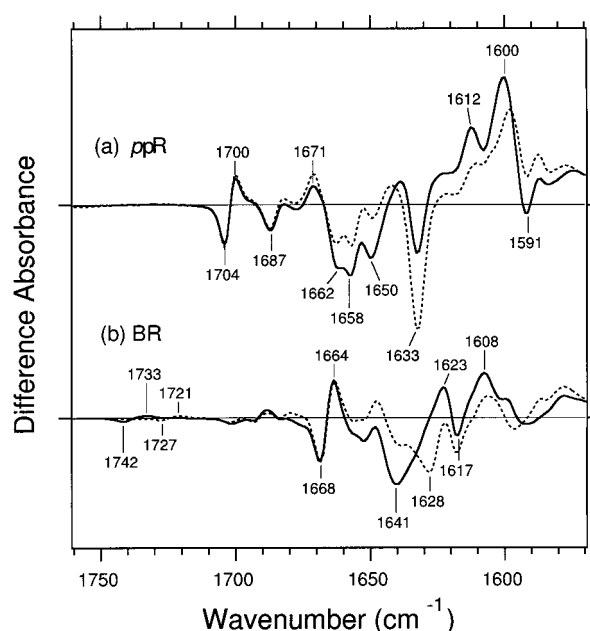


FIGURE 1: *ppR*_K minus *ppR* (a) and BR_K minus BR (b) spectra measured in the 1760–1570 cm^{-1} region at 77 K. The sample was hydrated with either H₂O (—) or D₂O (···). One division of the Y-axis corresponds to 0.008 absorbance unit. The spectra are reproduced from ref 14.

K. Illumination conditions for *ppR* were identical to those reported previously: 450 nm light for the *ppR* to *ppR*_K conversion and >560 nm light for the *ppR*_K to *ppR* reversion (14). Illumination conditions for BR were as described previously: 501 nm light for the BR to BR_K conversion and >660 nm light for the BR_K to BR reversion (20). The difference spectrum was calculated from the spectra constructed with 128 interferograms before and after the illumination. Twenty-four spectra obtained in this way were averaged for the *ppR*_K minus *ppR* and BR minus BR spectra. Linear dichroism experiments revealed a random orientation of the *ppR* molecules and highly oriented BR molecules in the film. Therefore, an IR polarizer was not used in the measurements for *ppR*, while polarized measurements with a window tilting angle of 53.5° were applied for BR (20).

RESULTS

Assignment of a Characteristic Vibrational Band of ppR as the C=O Stretch of Asn105. Figure 1 compares the IR difference spectra at 77 K between *ppR* (a) and BR (b); these results are reproduced from Kandori et al. (14). Various protein bands appear in this frequency region in addition to the C=N stretch of the Schiff base. Greater spectral changes are characteristic for *ppR* compared to BR, suggesting that more extended protein structural changes occur in *ppR*. These changes are coincident with the spectral feature of hydrogen out-of-plane (HOOP) vibrations in the K intermediate (14). That is, the strong peaks of the HOOP bands in BR_K were localized in the Schiff base region, whereas many more peaks were observed in *ppR*_K (14). These facts indicate that the structural changes are localized around the Schiff base region in BR as was also shown by an X-ray crystallographic study of BR_K (21), while changes are more extended in *ppR*_K. The previous FTIR study also suggested that the local structure at positions C10 and C11 of the retinal chromophore are similar in BR and *ppR*, but different in BR_K and *ppR*_K (14).

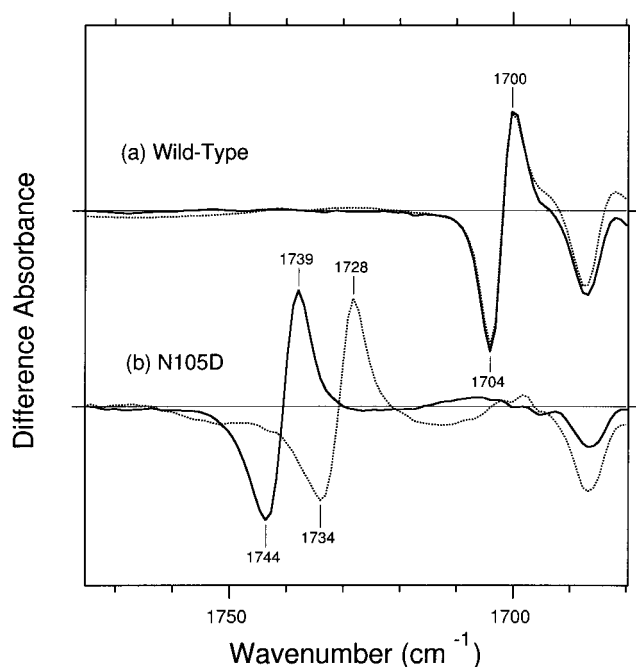


FIGURE 2: ppR_K minus ppR spectra in the 1775–1680 cm^{-1} region of the wild type (a) and N105D (b). The sample was hydrated with either H_2O (—) or D_2O (···). One division of the Y-axis corresponds to 0.0015 absorbance unit.

Among the various bands in Figure 1, a characteristic difference is seen in the 1750–1700 cm^{-1} region. In BR, the 1742(–)/1733(+) cm^{-1} bands in H_2O are shifted to 1727(–)/1721(+) cm^{-1} in D_2O (Figure 1b), which was previously assigned as the C=O stretch of Asp115 (22). The corresponding amino acid is Asn105 in ppR , so no spectral changes are observed in the 1750–1710 cm^{-1} region of ppR (Figure 1a). In contrast, sharp peaks are observed at 1704(–) and 1700(+) cm^{-1} in ppR , which do not change their frequencies in D_2O . The origin of the bands may be the C=O stretch of the peptide backbone (amide I vibration), though the frequencies are considerably higher than that of the typical amide I vibration. On the other hand, the bands may be ascribable to the C=O stretching vibration of asparagine, because the amino acid corresponding to Asp115 of BR (Figure 5b) is Asn105 in ppR . Thus, we prepared the N105D mutant protein, and applied low-temperature FTIR spectroscopy. The N105D protein possessed an absorption spectrum identical to that of the wild type in DM solution, the absorption maximum of which was at 500 nm (data not shown).

Figure 2 clearly shows that the 1704(–)/1700(+) cm^{-1} bands in the wild type disappeared in N105D. On the other hand, the 1744(–)/1739(+) cm^{-1} bands newly appeared in N105D, both of which are downshifted by 10–11 cm^{-1} in D_2O . As shown below, spectra in other frequency regions are very similar between the wild-type and N105D proteins, indicating that the spectral modification does not originate from a secondary effect of the mutation. Thus, we assigned the bands at 1704 and 1700 cm^{-1} as the C=O stretching vibrations of Asn105 in ppR and ppR_K , respectively. Similarly, the bands at 1744 and 1739 cm^{-1} can be assigned as the C=O stretching vibrations of protonated Asp105 in the N105D mutant and its K intermediate, respectively.

Spectral Characteristics of C=O Stretching Vibrations of Asparagine and Aspartic Acid in ppR and BR. Asn105 in

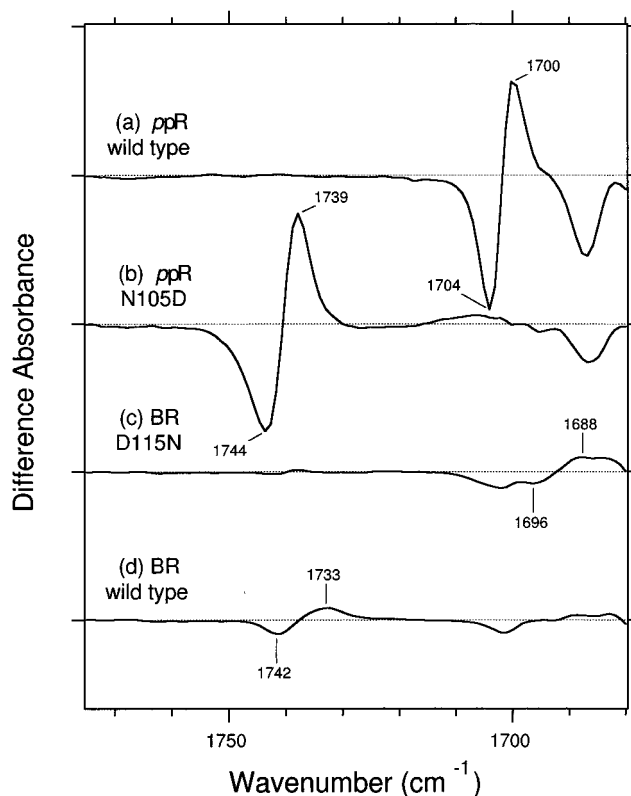


FIGURE 3: ppR_K minus ppR spectra of the wild type (a) and N105D (b) and BR_K minus BR spectra of D115N (c) and the wild type (d) measured in the 1775–1680 cm^{-1} region. One division of the Y-axis corresponds to 0.0012 absorbance unit.

ppR corresponds to Asp115 in BR, and both side chains change their structures upon photoisomerization. Lower-frequency shifts upon K formation (Figure 1) indicate stronger hydrogen bonds of the C=O groups for Asn105 in ppR and Asp115 in BR. Figure 1 also shows a notable difference in the amplitude of the C=O bands between ppR and BR. The greater amplitude in ppR compared to that in BR may suggest a difference in their structural changes upon photoisomerization. Therefore, we next systematically compared difference spectra of four species as shown in Figure 3: ppR possessing Asn105 (wild type) (a) and Asp105 (b) and BR possessing Asn115 (c) and Asp115 (wild type) (d).

For ppR , the 1704(–)/1700(+) cm^{-1} bands (Figure 3a) are the C=O stretches of Asn105 while the 1744(–)/1739(+) cm^{-1} bands (Figure 3b) are the C=O stretches of protonated Asp105. For BR, the 1742(–)/1733(+) cm^{-1} bands (Figure 3d) are the C=O stretches of protonated Asp115, which disappeared in the D115N mutant (Figure 3c). On the other hand, the 1696(–)/1688(+) cm^{-1} bands newly appeared in the D115N mutant, which was also observed in the BR_L minus BR spectrum of the mutant (23).

Thus, the frequencies of the C=O stretch of asparagine were at 1704 and 1696 cm^{-1} in ppR and BR, respectively, while those of the C=O stretch of protonated aspartic acid were at 1744 and 1742 cm^{-1} in ppR and BR, respectively. The difference in frequency of 40–50 cm^{-1} between asparagine and aspartic acid originates from the vibrational properties of their groups (24). Coincidence in frequencies for the same residues in ppR and BR implies that the residues

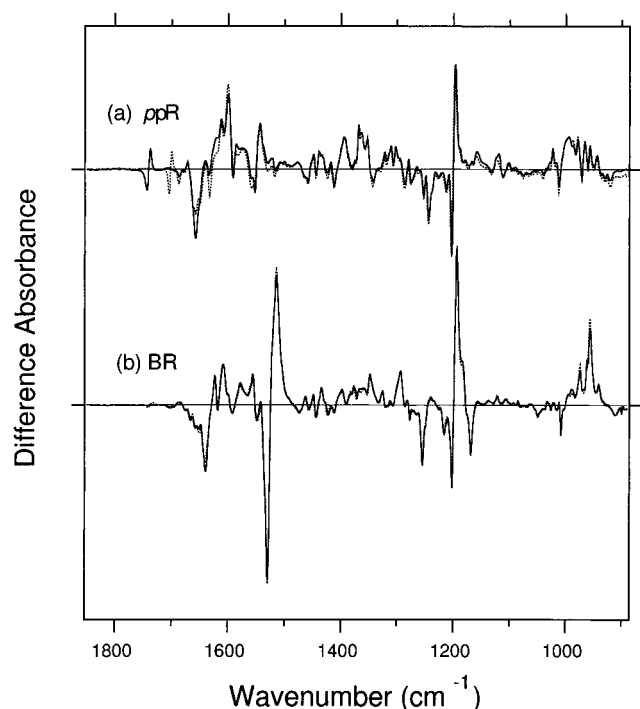


FIGURE 4: ppR_K minus ppR spectra of the wild type [a (···)] and N105D [a (—)] and BR_K minus BR spectra of the wild type [b (···)] and D115N [b (—)] measured in the 1850–890 cm^{-1} region. One division of the Y-axis corresponds to 0.01 absorbance unit.

are in a similar environment in both proteins. In addition, all spectra exhibit lower-frequency shifts of the $\text{C}=\text{O}$ stretches upon formation of the K intermediates (Figure 3), indicating that the hydrogen bonds of the $\text{C}=\text{O}$ groups become stronger upon photoisomerization.

Despite these similarities, the difference in amplitude of the $\text{C}=\text{O}$ bands was preserved between *ppR* and *BR*. Figure 3 shows that the amplitude is ~ 10 times greater in *ppR* than in *BR*, regardless of asparagine or aspartic acid being at the corresponding position. Figure 4 shows the spectra of Figure 3 in the 1850–890 cm^{-1} region. It is noted that the spectral comparison is not completely quantitative between *ppR* and *BR* under the present experimental conditions. However, visible absorbances of *ppR* and *BR* are comparable. In addition, a difference in amplitude of the $\text{C}=\text{O}$ stretches is clear between *ppR* and *BR*, where negative bands at ~ 1255 , ~ 1203 , and ~ 1010 cm^{-1} are comparable in amplitude. *ppR* molecules are randomly distributed in the hydrated film, while *BR* molecules are highly oriented (the sample film was thereby tilted by 53.5°). However, the previous polarized FTIR spectroscopy of *BR* revealed that the $\text{C}=\text{O}$ group of Asp115 is oriented by 50 – 60° to the membrane normal (25), indicating that the small amplitude in *BR* is not because of its dichroic properties.

Figure 4 shows a tiny effect of mutation. In *BR*, difference spectra are almost identical for the wild-type (dotted line) and D115N mutant (solid line) proteins except for the 1750–1680 cm^{-1} region (Figure 3c,d). Both spectra also look similar in *ppR* (Figure 4a). It is, however, noted that spectral deviation conferred by mutation is considerably larger in *ppR* than in *BR*. This fact could be correlated with the greater amplitude of the $\text{C}=\text{O}$ stretches at position 105 in *ppR* (position 115 in *BR*) in the difference spectrum.

DISCUSSION

*Environment of Asn105 in *ppR* and Asp115 in *BR* before and after Photoisomerization.* The FTIR spectroscopy results presented here assigned the $\text{C}=\text{O}$ stretching vibration of Asn105 in the ppR_K minus ppR difference spectrum. It is noted that the $\text{C}=\text{O}$ stretch of protonated aspartic acids is highly sensitive to their hydrogen bonding conditions, and the corresponding frequencies occur in the 1780–1700 cm^{-1} region (26). The frequency at 1744 cm^{-1} of the N105D mutant of *ppR* is very close to that of Asp115 in *BR* (1742 cm^{-1}), indicating that both $\text{C}=\text{O}$ groups form moderate hydrogen bonds. Frequencies of the $\text{C}=\text{O}$ group of asparagine (Asn105 of *ppR* and Asn115 of *BR*) are also close to each other (1704 and 1696 cm^{-1} , respectively). These facts imply a structural similarity of the corresponding position in *ppR* and *BR*. Thus, we concluded that the local structure of position 105 in *ppR* is similar to that of position 115 in *BR*.

Despite structural similarity in the ground states of *ppR* and *BR*, there is a definite difference in the difference spectra of the K intermediates. The amplitude of the $\text{C}=\text{O}$ stretch band in the difference spectra was ~ 1 order of magnitude greater in *ppR* than in *BR*. The smaller amplitude in *BR* is not the property of the $\text{C}=\text{O}$ group itself, because a more than 5-fold greater amplitude was observed for the negative 1742 cm^{-1} band (Figure 1b) in the BR_{MN} minus BR spectrum of the D96N mutant (H. Kandori, unpublished observation). Therefore, the most straightforward interpretation is that the spectral shift of the $\text{C}=\text{O}$ stretch is larger in *ppR* than in *BR*. The structural changes at position 105 in *ppR* are likely to be greater than those at position 115 in *BR* upon photoisomerization. This conclusion is consistent with the previous observation that protein structural changes are more extended in *ppR* than in *BR* in view of chromophore distortion and peptide backbone vibrations (14).

*Implication from Crystallographic Structures of *BR* and *ppR*.* Figure 5a shows the X-ray crystallographic structure of *BR* (27), where Asp115 is shown together with possible hydrogen-bonding partners and the retinal chromophore. Asp115 in helix D does not directly interact with the retinal chromophore. The nearest atom in the chromophore from one of the side chain oxygens of Asp115 (OD2) is the ninth methyl carbon (6.4 Å). The other atoms within 7 Å are C9, C10, and C11 at the central part of the chromophore (Figure 5). There are no hydrogen-bonding partners around OD2. Another oxygen atom of Asp115 (OD1) is located within possible hydrogen bonding distance of Thr90 (2.4 Å) and water511 (3.1 Å).

Although the structure of *ppR* was not known at the start of our work, X-ray crystallographic structures of *ppR* have been reported by two groups after our writing of this paper (28, 29). Figure 5b shows one of the X-ray crystallographic structures of *ppR* (28), where Asn105 is shown together with possible hydrogen-bonding partners and the retinal chromophore. The side chain $\text{C}=\text{O}$ group of Asn105 interacts with Thr80 and water602 (Figure 5b), as does OD1 of Asp115 with Thr90 and water511 (Figure 5a). The similar environments of Asp115 in *BR* and Asn105 in *ppR* are consistent with these FTIR results. The slightly longer distance between Asn105 and Thr80 in *ppR* may be related to the higher frequencies in *ppR* (Figure 3), because a higher frequency corresponds to a weaker hydrogen bond.

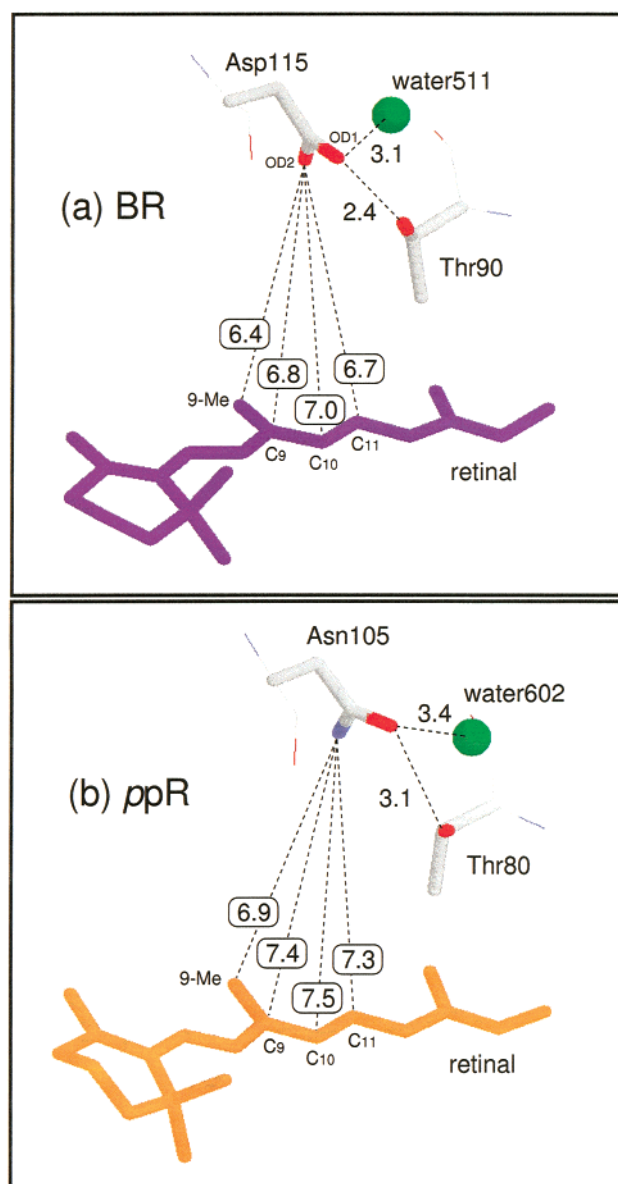


FIGURE 5: (a) Distance between Asp115 and the retinal chromophore according to the X-ray structure of BR (27). Four atoms of retinal are labeled that are located within 7 Å of one of the side chain oxygens of Asp115 (OD2). Another oxygen atom of Asp115 (OD1) is located within possible hydrogen bonding distance of Thr90 (2.4 Å) and water511 (3.1 Å). (b) Distance between the side chain nitrogen of Asn105 and the corresponding four atoms of the retinal chromophore (9-Me, C9, C10, and C11) shown according to the X-ray structure of ppR (28). The side chain oxygen atom of Asn105 is located within possible hydrogen bonding distance of Thr80 (3.1 Å) and water602 (3.4 Å).

The distance between Asn105 and the retinal chromophore indicates no direct interaction in ppR (Figure 5b). Interestingly, the distance is slightly longer in ppR than in BR. The nearest atom in the chromophore from the side chain nitrogen of Asn105 is the ninth methyl carbon (6.9 Å). All other atoms are located at a distance of >7 Å (Figure 5b). Thus, the present FTIR spectroscopy results clearly indicate that retinal isomerization accompanies extended protein structural changes into the region of Asn105 in ppR. Structural changes appear to reach further away from the isomerization site in ppR.

It is not clear at this moment why protein structural changes upon photoisomerization are more extended in ppR

than in BR. The primary reaction rate (30) and product formation yield of ppR (31) are comparable to those of BR, implying that the potential surfaces of the excited states are similar between them. Thus, the difference in the K structures seems to originate from a refined correlation of structure and dynamics. It is likely that the difference in amino acids surrounding the retinal chromophore is mainly localized around the β -ionone ring, those in helices D (Asn105, Val108, and Met109 in ppR) and E (Phe127, Gly130, Ala131, and Phe134 in ppR). These amino acids, including Asn105, must be closely related to the specific interaction of ppR upon K formation. Although the Schiff base region, the other end of the retinal chromophore, is highly conserved between ppR and BR, a stronger hydrogen bond of the Schiff base was observed in ppR than in BR (14, 32, 33). We infer that both the β -ionone ring and the Schiff base regions contribute the unique chromophore–protein interaction in ppR, and this leads to the extended protein structural changes accompanying retinal photoisomerization.

ACKNOWLEDGMENT

We thank M. Iwamoto and Y. Sudo for helping in sample preparation and Y. Furutani for helping in infrared spectroscopy. We also thank Dr. R. Needleman for providing the D115N mutant strain of BR and improving the manuscript.

REFERENCES

1. Sasaki, J., and Spudich, J. L. (2000) *Biochim. Biophys. Acta* 1460, 230–239.
2. Kamo, N., Shimono, K., Iwamoto, M., and Sudo, Y. (2001) *Biochemistry (Moscow)* 66, 1580–1587.
3. Spudich, J. L., and Lanyi, J. K. (1996) *Curr. Opin. Cell Biol.* 8, 452–457.
4. Imamoto, Y., Shichida, Y., Hirayama, J., Tomioka, H., Kamo, N., and Yoshizawa, T. (1992) *Biochemistry* 31, 2523–2528.
5. Takahashi, T., Yan, B., Mazur, P., Derguini, F., Nakanishi, K., and Spudich, J. L. (1990) *Biochemistry* 29, 8467–8474.
6. Miyazaki, M., Hirayama, J., Hayakawa, M., and Kamo, N. (1992) *Biochim. Biophys. Acta* 1140, 22–29.
7. Imamoto, Y., Shichida, Y., Hirayama, J., Tomioka, H., Kamo, N., and Yoshizawa, T. (1992) *Photochem. Photobiol.* 56, 1129–1134.
8. Hirayama, J., Imamoto, Y., Shichida, Y., Kamo, N., Tomioka, H., and Yoshizawa, T. (1992) *Biochemistry* 31, 2093–2098.
9. Engelhard, M., Scharf, B., and Siebert, F. (1996) *FEBS Lett.* 395, 195–198.
10. Schmies, G., Luttenberg, B., Chizhov, I., Engelhard, M., Becker, A., and Bamberg, E. (2000) *Biophys. J.* 78, 967–976.
11. Sudo, Y., Iwamoto, M., Shimono, K., Sumi, M., and Kamo, N. (2001) *Biophys. J.* 80, 916–922.
12. Schmies, G., Engelhard, M., Wood, P. G., Nagel, G., and Bamberg, E. (2001) *Proc. Natl. Acad. Sci. U.S.A.* 98, 1555–1559.
13. Kunji, E. R. S., Spudich, E. N., Grishammer, R., Henderson, R., and Spudich, J. L. (2001) *J. Mol. Biol.* 308, 279–293.
14. Kandori, H., Shimono, K., Sudo, Y., Iwamoto, M., Shichida, Y., and Kamo, N. (2001) *Biochemistry* 40, 9238–9246.
15. Shimono, K., Iwamoto, M., Sumi, M., and Kamo, N. (1997) *FEBS Lett.* 420, 54–56.
16. Shimono, K., Kitami, M., Iwamoto, M., and Kamo, N. (2000) *Biophys. Chem.* 87, 225–230.
17. Needleman, R., Chang, M., Ni, B., Varo, G., Fornes, J., White, S. H., and Lanyi, J. K. (1991) *J. Biol. Chem.* 266, 11478–11484.
18. Oesterholt, D., and Stoekenius, W. (1973) *Methods Enzymol.* 31, 667–678.

19. Kandori, H., and Maeda, A. (1995) *Biochemistry* 34, 14220–14229.
20. Kandori, H., Kinoshita, N., Shichida, Y., and Maeda, A. (1998) *J. Phys. Chem. B* 102, 7899–7905.
21. Edman, K., Nollert, P., Royant, A., Belrhali, H., Pebay-Peyroula, E., Hajdu, J., Neutze, R., and Landau, E. M. (1999) *Nature* 401, 822–826.
22. Braiman, M. S., Mogi, T., Marti, T., Stern, L. J., Engel, F., Khorana, H. G., and Rothschild, K. J. (1988) *Biochemistry* 27, 8516–8520.
23. Maeda, A., Sasaki, J., Shichida, Y., Yoshizawa, T., Chang, M., Ni, B., Needleman, R., and Lanyi, J. K. (1992) *Biochemistry* 31, 4684–4690.
24. Lin-Vien, D., Colthup, N. B., Fateley, W. G., and Grasselli, J. G. (1991) *The Handbook of Characteristic Frequencies of Organic Molecules*, Academic Press, San Diego.
25. Kandori, H. (1998) *J. Am. Chem. Soc.* 120, 4546–4547.
26. Maeda, A. (1995) *Isr. J. Chem.* 35, 387–400.
27. Luecke, H., Schobert, B., Richter, H.-T., Cartailier, J. P., and Lanyi, J. K. (1999) *J. Mol. Biol.* 291, 899–911.
28. Luecke, H., Schobert, B., Lanyi, J. K., Spudich, E. N., and Spudich, J. L. (2001) *Science* 293, 1499–1503.
29. Royant, A., Nollert, P., Edman, K., Neutze, R., Landau, E. M., Pebay-Peyroula, E., and Navarro, J. (2001) *Proc. Natl. Acad. Sci. U.S.A.* 98, 10131–10136.
30. Lutz, I., Sieg, A., Wegener, A. A., Engelhard, M., Boche, I., Otsuka, M., Oesterheld, D., Wachtveitl, J., and Zinth, W. (2001) *Proc. Natl. Acad. Sci. U.S.A.* 98, 962–967.
31. Losi, A., Wegener, A. A., Engelhard, M., Gartner, W., and Braslavsky, S. E. (1999) *Biophys. J.* 77, 3277–3286.
32. Gellini, C., Luttenberg, B., Sydor, J., Engelhard, M., and Hildebrandt, P. (2000) *FEBS Lett.* 472, 263–266.
33. Kandori, H., Furutani, Y., Shimono, K., Shichida, Y., and Kamo, N. (2001) *Biochemistry* 40, 15693–15698.

BI0120749